

# Study on estimating tree height distribution using the polarimetric interferometric PALSAR data analysis

PI-193

Masanobu Shimada, Takeo Tadono, and Masato Ohki

Earth Observation Research and application Center (EORC), Japan Aerospace and Exploration Agency, (JAXA) Sengen 2-1-1, Tsukuba, Ibaraki, Japan, 305-8505, Voice 81-29-868-2474, Fax: 81-29-868-2961, [shimada.masanobu@jaxa.jp](mailto:shimada.masanobu@jaxa.jp)

**Abstract** PALSAR PolInSAR capability was evaluated. One of the important capabilities that the PolInSAR offers is to estimate the forest height. For one-year and more months after the launch of the ALOS on Jan. 24 2006, PLASAR observed several test areas using the polarimetry modes repeatedly. We applied the PolInSAR method to retrieve the forest heights of the four test sites in Japan and Amazon. In this paper, we introduce an applied method and results. The results show that the forest tree height can be estimated with good accuracy.

## I. INTRODUCTION

While PALSAR offers several modes for operation, polarimetric mode is the world first operational one prepared for the spaceborne segment. Thus, the data collection is required world widely on the methodology demonstration purpose. As for the full polarimetric mode, PALSAR offers 12 mode selections, which mainly varies with the off nadir angle from 7.7 degrees to 26.1 degrees. Since Polarimetry mode needs the double pulse repetition frequency more than the FBS (Fine Beam SiNgle) or FBD (Fine Beam Dual), the imaging swath is reduced to be a half of the normal swath of 70 km. For the operational ease, 21.5 degrees is selected as the operational polarimetry mode. Some of the rested modes were activated for the calibration and the urgent observation purpose, and the

remained have not been used at all. The calibration accuracy of polarimetric modes is rather stable and the accuracy is excellently well maintained [1]. The one-year monitoring results show the excellent stability and thus the calibration factor should not be updated. The phase balance of VV/HH after calibration has 0.3 degree with the standard deviation of 1.0 degree, and amplitude of 0.02 dB, separately. Here, the CEOS SAR CAL/VAL group required 5 degree for the phase balance and 0.2 dB for amplitude balance. Thus, the PALSAR meets the CESO SAR requirement. Noise equivalent sigma zero is measured as -27 dB from the Amazon River and that cross talk is -34 dB [5]. Thus, the PALSAR polarimetry shows the quite accurate performances. Here, we will discuss of the PolInSAR application that ALOS can do in this paper (Table 1 shows the PALSAR polarimetric characteristics). With regard to the forest height estimations, many approaches have been developed [2], [3]. Basic idea is to maximize the differential heights, which is observed interferometrically using the different polarizations and L-band SAR, which has penetration capability to the forest canopy. When SAR is operated using two polarizations in transmission and reception, the four transmit-reception phase combinations express the penetration depths depending on the forest structure.

H transmit and H receive has double bounce from the ground and the tree bottom and the tree canopy. HV has less penetration but large diffuse scattering from the forest canopy. VV has large backscattering from the forest canopy and small from the tree trunks. Dealing the four scattering component interferometrically, the height of the trees can be derived. But the problem is that the PALSAR has 46 days repeat cycle and temporal decorrelation can be a problem on deriving the phase information. Thus the coherence dependence on the forest type is one of the interests on knowing if the tree height estimation can be conducted. Here, we collected tow images pairs from the Amazon, which is supposed to be a dense forest mainly or sparsely, and two image pairs from Japan's typical forest at Tomakomai and mountainous forest in Kanto district. Here, we will show a trial to estimate the forest height using the PALSAR PolInSAR approach.

Signal in Table 1 PALSAR Polarimetric characteristics

Center Frequency	1.270GHz
Bandwidth	14.0MHz
Sampling frequency	16.0 MHz
Pulse width	16.0 micro sec.
A/D bits	5 I and 5 Q
Transmission power	2Kw

Keywords PALSAR, ALOS, Polarimetric mode

## II. Height estimation

For a pair of the PALSAR polarimetric images whose perpendicular baseline is less than the critical baseline, the covariance matrix gives a complex component equation for the polarimetric interferometry data.

$$C_{ij} = \frac{\langle m_i \cdot s_j^* \rangle}{\sqrt{\langle m_i \cdot m_j^* \rangle \langle s_i \cdot s_j^* \rangle}} \quad (1)$$

$$= \exp(j\phi_{ij}) \frac{\tilde{\gamma}_v + m_{ij}}{1 + m_{ij}}$$

$$m_i = [m_{HH} + m_{VV}, m_{HH} - m_{VV}, m_{HV} + m_{VH}] \quad (2)$$

$$s_j = [s_{HH} + s_{VV}, s_{HH} - s_{VV}, s_{HV} + s_{VH}]$$

where, the suffix i, and j shows the Pauli basis notation and each one means that 1 for HH+VV, 2 for HH-VV, and 3 for HV+VH, and all are calibrated using the distortion matrix shown in [1]. m and s means the master and the slave image and  $\langle \rangle$  means the ensemble average. Here, 2 looks in range and 16 looks in azimuth are average. Complex covariance matrix (coherence matrix) is a 3x3 complex component and is non-Hermitian. Second expression in (1) shows an explicit expression between each term of the Cij and the coherence contribution in each polarization [2].  $m_{ij}$  is the ground to volume mass ratio in the ij combination.  $\gamma$  is the coherence of the volume scattering, and  $\phi$  is the interferometric phase.

The characteristic equation of the (1) gives three complex Eigen values ( $\lambda_k$ ) and Eigen vectors ( $v_k$ ) as.

$$C_{ij} = \lambda_1 v_1 + \lambda_2 v_2 + \lambda_3 v_3 \quad (3)$$

$$|\lambda_1| > |\lambda_2| > |\lambda_3|$$

where, Eigen values express three representative scattering points in Pauli bases. Scatterers are composed of odd scatterers (surface, sphere, flat surface, and multiple odd scatterings), and even scatterers (double bounce, multiple even scatterers), and volume scatters. When the target is made of only one component, i.e., surface, RANK of the target is one (see Fig.1 for the scattering mechanism introduction). Thus the rank can be used for the target description. Eigen value was calculated using the Eispack

[4].

For the RANK 1 target, discrimination of the river and the rough surface can be based on the sigma-naught difference that the sigma-naught lower than -20 dB should indicate the river and if not it could be the rough surface.

Differentiation of the Eigen values can be converted to the height of the target.

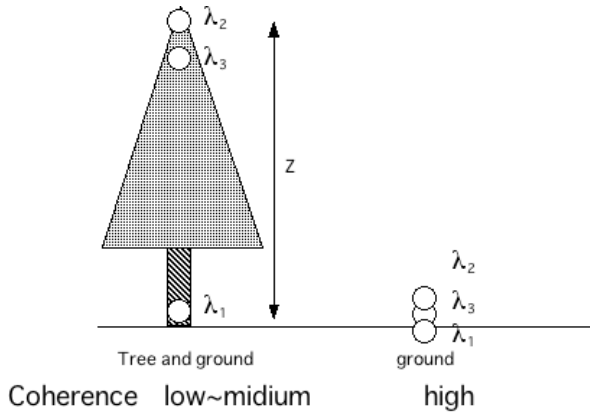


Fig. 1 Scattering mechanism of the target is shown. Left shows that three Eigen values distribute representing the main scattering mechanism (double bounce, volume scattering, and surface scattering) and right shows three Eigen values collapse on the ground, which is because that the scattering mechanism is only one.

$$z = \frac{\lambda}{4\pi} \frac{r \cdot \sin\theta}{B_p} \phi \quad (4)$$

$$\phi = \arg(\lambda_1, \lambda_2) \text{ or } \arg(\lambda_1, \lambda_3) \quad (5)$$

where,  $\lambda$  is the wavelength, 23.6 cm,  $r$  is the slant range,  $B_p$  is the perpendicular baseline, and  $\theta$  is the incidence angle at the earth ellipsoid.

### III. EXPERIMENTS

#### 3-1) Data acquisitions

The resource assignment to the polarimetry mode of the PALSAR was only 7% of whole PALSAR capability. This is because that the main PALSAR user is disaster

mitigation using FBS and forest monitoring using FBD.

Extension of the resource allocation to polarimetry mode needs more time and demonstration. Two consecutive operations of the PALSAR polarimetric modes every other year may not prove the PolInSAR capability so much. Other than this, the several test sites have been already set during the calibration phase from May 16 2006 to Oct 23 2006. We used four datasets selected from these sites, which are the Tomakomai sites and the Amazon test sites. Although the L band SAR is easily affected by the ionospheric perturbation on Faraday rotation and the range distortion, we used the data without correction. Table 2 shows a list of the image pair used in this analysis.

Table 2 Image pairs evaluated in this analysis

Area	Obs date	Obs date	Bp	A/D
Amazon1/Brazil	10/20/2006	9/4/2006	-196m	A90
Amazon2/Brazil	10/21/2006	9/5/2006	-199m	A431
Tomakomai/Japa	10/4/2006	8/19/2006	1048m	D
Kanto/Japan	10/21/2006	9/5/2006	249m	D63

#### 3-2) Evaluation and discussions

We introduce two examples one from Amazon and one from Japan forest below. All the data are expressed in the slant range image (in horizontal direction) and azimuth (vertical) direction below. The orbit is maintained within the diameter of 500 meter. Thus the most of the example in Table 2 meets this requirement.

#### 3-3) Amazon Dense Forest

The image locates at latitude of -9.7 degrees and -67 degrees, west of the Amazon and almost on the geomagnetic equatorial region. Each image size is 35 km in both range and azimuth directions. As the image is shown in Fig.2, area is mixed with the dense forest, which looks gray, and clear-cut area which looks dark. As seen from this image, HV+VH has more contrast than HH+VV

and HH-VV. As a reference, we show Fig.3 as the HV basis images of HH, HV, and VV. HH+VV represents the odd number scattering; HH-VV does for the even scattering, and HV+VH for the random scattering. More contrast in HV+VH means that the low vegetation in the clear-cut (may include young trees) area can not been observed by the cross polarization, while the even and odd number scattering have sensitivity to the like pol. scattering.

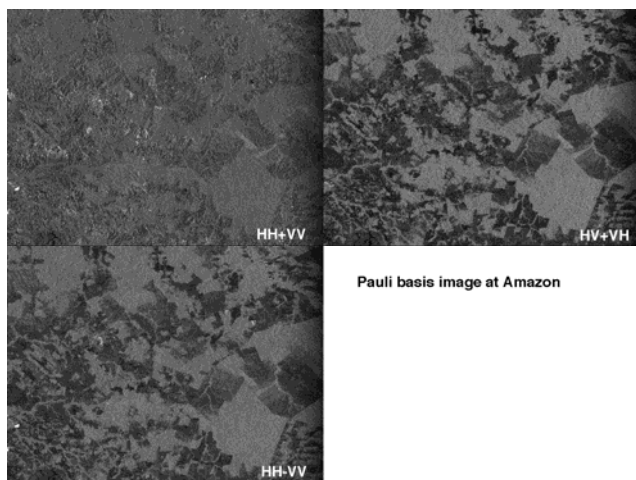


Fig. 2 Comparison of the three amplitude images, left top is HH+VV, right top is HV+VH, and left bottom is HH-VV. Before summation, the data are polarimetrically calibrated. Clear contrast in HV+VH is because the young tree in the cut area is less response in this polarization. Similar contracts in the HH-VV are slightly different from the above. It is due to that the brighter are has larger double bounce and dark area has smaller one.

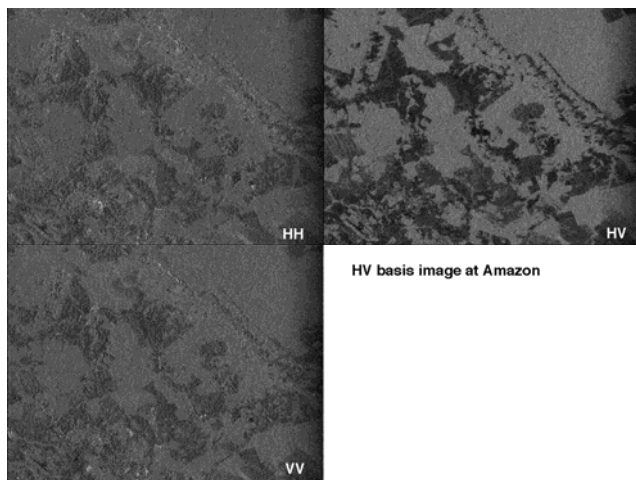


Fig. 3 Comparison of the three linear basis images, left top is HH, right top is HV and left bottom is VV. All images are polarimetrically calibrated.

Coherence images are shown in Fig. 4 in the same basis order as previous figures. HH+VV has the biggest coherence among three orthogonal combinations. The other two are reduced so much. This is due to that the total power of HH+VV exceeds than the others.

Most of this case shows that three Eigen values are categorized in two bigger Eigen values and one quite smaller Eigen value. This tendency appears in dense forest and clear-cut, where the target is unknown whether it is clearly cutout or still including the young trees. This means that most of the scattering properties are represented by two main points. In (5), angular difference are mostly selected as first and second Eigen values.

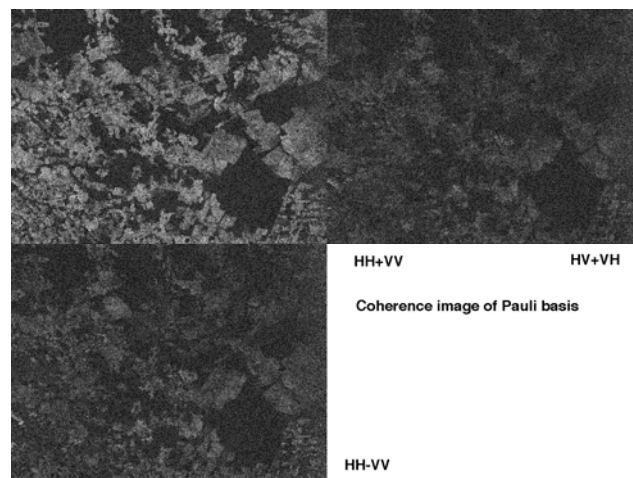


Fig. 4 Coherence comparison among the three basis of the Amazon is shown. The coherence in HH+VV is high in the clear-cut area or low vegetation area. HV+VH and HH-VV are almost similar but slight difference is observed. It may be due to the difference of the scattering mechanism.

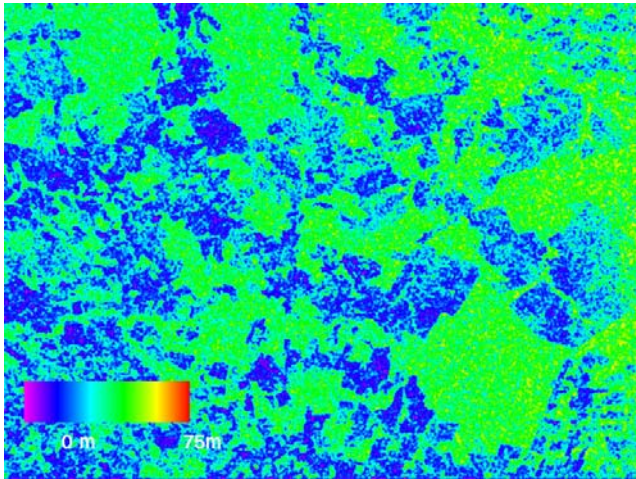


Fig. 5 Forest height derived from the PolInSAR processing. Averaged height of the region A is 40m.

### 3-4) Mountain forest in Japan

We selected the second test area from the Kanto flat plane in Japan. Fig. 6 shows the amplitude image of the target area, where HV+VH are displayed. Upper half is the mountainous area of 400m height and the lower half is flat area including two rivers running x directions.

The coherence of the image is very high. While we show one example of HH+VV in the Fig. 7, all the other orthogonal image pairs show high coherence. And, the non-orthogonal pair shows almost zero coherence. This means that all the images can be well calibrated polarimetrically as the way that the crosstalk is due to the Faraday rotation. In this image, the mountain site has medium high, quite high at the flat area, and dark at the river or the flat area.

Forest height distribution is given in Fig. 8 with the color code. Averaged tree height in this image is 10m in the mountainside. The river colored in green seems ambiguous.

Simple interferometry in the HH+VV gives the height information where the one color cycle is 145m and the mountain in this image has 400m-peak height.

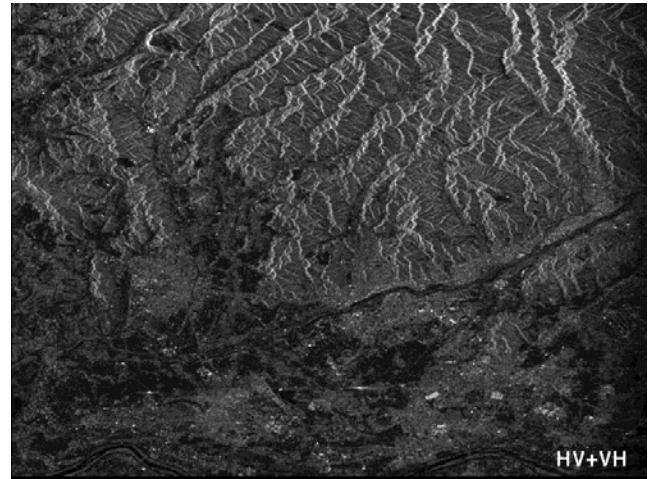


Fig. 6 Amplitude image of the target area is shown in cross pol mode for showing the forest site (gray means the diffuse scattering of the forest). White are shows the forest area, and the dark area shows the low vegetation of the rivers.

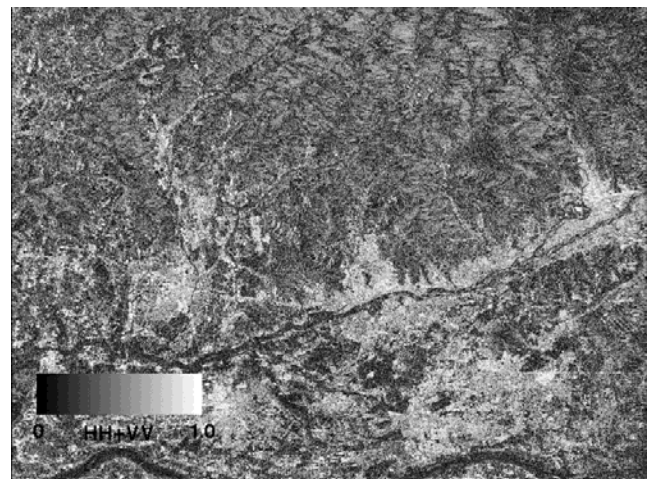


Fig. 7 Coherence of the HH+VV, one of the Pauli bases, is introduced.

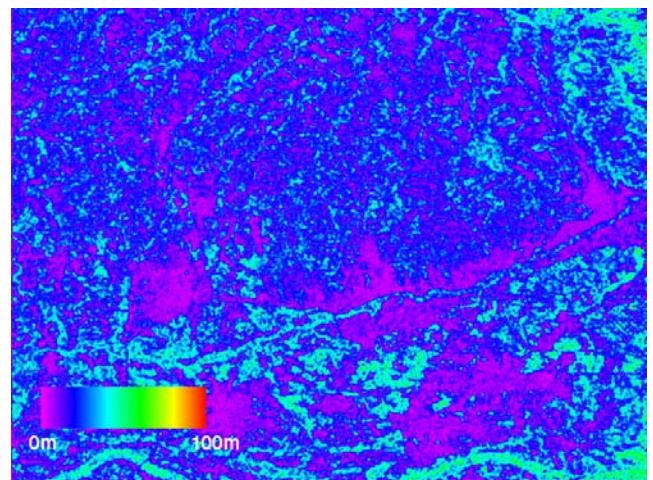


Fig. 8 Forest height distribution map is colored in the range of the 100m. Most of the area looks the color of 10m

except the river (green), which is ambiguous.

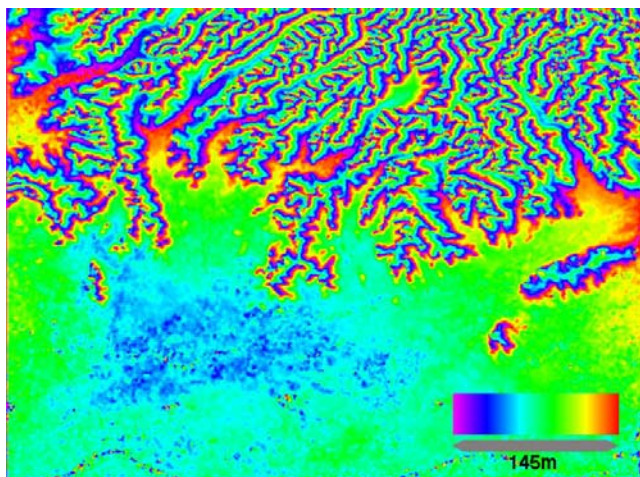


Fig. 9 Interferometric height distribution of the target area is shown in the color code of 145 m span.

#### IV Discussion and Conclusions

In this paper, we showed the experimental results of obtaining the tree height distributions over the Amazon rain forest and the Japan's mountain forest. Both results showed the reasonable values on the tree height, which are 40 meter in Amazon and 10 meter in Japan forest. We have not quantitatively evaluated the results. In the next phase, we will evaluate the results using the Tomakomai forest in Japan where ground truth data were collected well enough. Algorithm improvement will be conducted in a way that the selection of the Eigen values expressing the ground target. More improvement is to clarify the meaningful separation of two bigger Eigen values often observed in the single target or the river.

#### Acknowledgement

The author expresses sincere thanks all the people contributed to develop the PALSAR and its operation.

#### References

- [1] M. Shimada et al, "PALSAR CALVAL Summary and Update 2007," Proc. of IGARSS07, Barcelona, Spain, 2007.
- [2] K. Papanassiou, "Polarimetric SAR Interferometry for Quantitative Parameter Estimation - The key challenge focusing Synthetic Aperture Radar (SAR) remote sensing from high-resolution imaging to high-resolution accurate measurement," CCG seminar SE 2.06-SAR principle and Applications Oct 24-28, 2005, Oberpfaffenhofen, Germany
- [3] S. R. Cloud, and K. P. Papathanassiou, "Polarimetric SAR Interferometry," IEEE, Trans. Geoscience and remote sensing, Vol.36, No.5, Sept 1998, pp. 1551-1565.
- [4] Eispack, <http://epp.eps.nagoya-u.ac.jp/num-analysis/eispack.html>
- [5] M. Shimada, O. Isoguchi, T. Tadono, and K. Isono, "PALSAR Radiometric and Geometric Calibration," IEEE Trans. GRS, vol. 47, no. 12, pp.3915-3932, Dec 2009.